

Using SEST to Probe the Geometry of the Universe

P. ANDREANI, Dipartimento di Astronomia, Università di Padova, Italy

Many very interesting results in the field of observational Cosmology have been obtained in the past with the 15-m Swedish ESO Submillimetre Telescope (SEST) at La Silla (see the ESO/STC-148 Report on *Submillimetre Astronomy at ESO*).

The technical upgrades and improvements foreseen for SEST will undoubtedly boost projects in this field which, after a very successful start a few years ago, suffered a loss of competition with respect to other available sub-mm/mm facilities (i.e. IRAM, JCMT).

In view of the future development in the field of sub-mm/mm astronomy at ESO (see the leading article of this issue), the SEST antenna at La Silla will represent the most suited instrument to prepare projects and test instruments for the LSA/MMA arrays. A lot of work can be envisaged: for instance, deep surveys of small sky regions, aimed at looking for the long-sought dusty primeval galaxies, can be started with SEST.

An example of what has been done and hopefully *will* be pursued in the next future in the field of observational Cosmology is reported in this article.

1. The S-Z Effect and the Measure of H_0 and q_0

As already preliminarily described in *The Messenger* (No. 78, December 1994), a group of people (in alphabetic order: H. Böhringer, R. Booth, G. Dall'Oglio, R. Lemke, L. Martinis, L.-Å. Nyman, A. Otàrola, L. Pizzo, P. Shaver, N. Whyborn and myself) have started to use SEST to measure the Sunyaev-Zeldovich (S-Z) effect towards ROSAT clusters of galaxies.

The S-Z effect is one of the major sources of secondary anisotropies of the Cosmic Microwave Background (CMB), arising from (inverse) Compton scattering of the microwave photons by hot electrons in clusters of galaxies. This effect generates a peculiar signal with a decrement at wavelengths longer than 1.4 mm and an enhancement at shorter ones relative to the CMB planckian value. The original computation by Sunyaev and Zeldovich (1972) of the net transfer of energy from the hot e^- to the microwave photons predicts a signal for the relative temperature change:

$$\left(\frac{\Delta T}{T}\right)_{therm} = y \left(x \frac{e^x + 1}{e^x - 1} - 4\right) \quad (1)$$

where T is the CMB temperature, $x = hv/kT$ and $y = \int (kT_e/mc^2) n_e \sigma_T d\ell$ is the comptonisation parameter, n_e , T_e being the electron density and temperature.

If the cluster has a peculiar velocity relative to the frame where the CMB is isotropic an additional *kinematic* effect should be measured. The motion of the gas cloud will induce a Doppler change

whose relative amplitude, $\left(\frac{\Delta T}{T}\right)_{kin}$, does not depend on the frequency but only on the peculiar velocity, v_r , and cloud optical depth for Thomson scattering, τ ,:

$$\left(\frac{\Delta T}{T}\right)_{kin} = -\frac{v_r}{c} \tau$$

(where the minus sign refers to a cluster receding from the observer).

There is considerable interest in the detection of this effect also because of its potential in determining the distance and the peculiar and tangential velocities of clusters, and in studying the intra-cluster medium.

The physics of the effect is well understood, because it relies on properties of ionised gas in hydrostatic equilibrium. Furthermore, the effect does not depend on redshift, because of the luckily combination between the surface brightness dimming, $\propto (1+z)^{-4}$, and the increasing CMB energy density, $\epsilon_{CMB} \propto (1+z)^4$.

Here it is shown how it is possible to infer the cluster distance without using any secondary calibrators: the method is applicable to any individual source to any cosmological distance and does not depend on the evolutionary properties of the cluster as long as the physical state of the gas is understood. The basis consists of combining the S-Z effect measurements with X-ray data, since the X-ray surface brightness due to thermal bremsstrahlung, S_x , and the S-Z signal, ΔT_{SZ} , scale differently with n_e and a , the cluster core radius:

$$\Delta T_{SZ} \propto \langle n_e T_e \rangle a \quad (2)$$

$$S_x \propto \frac{V \langle n_e^2 \sqrt{T_e} \rangle}{D_l^2} \quad (3)$$

where V and D_l is the gas volume and the cluster luminosity distance, respectively. The combination of these measurements provide an estimate of a :

$$a \propto \Delta T_{SZ}^2 S_x^{-1} T_e^{-3/2} \frac{\theta^2}{(1+z)^4} \quad (4)$$

since a is related to the apparent angular size by the luminosity and angular diameter distance, D_A :

$$\frac{a}{\theta} = D_A = D_l (1+z)^{-2} \quad (5)$$

Therefore, measuring θ , ΔT_{SZ} , T_e , S_x and z gives D_A (D_l) and from it H_0 :

$$D_l = \frac{c}{q_0^2 H_0} \{z q_0 + (q_0 - 1) [-1 + \sqrt{1 + 2z q_0}]\} \quad (6)$$

Many groups in the world (mainly of radio astronomers) have successfully carried out so far observations of the Rayleigh-Jeans (R-J) decrement (see the recent review by Birkinshaw, 1997).

However, an unambiguous signature of the presence of the S-Z effect requires the measurement of both the decrement (negative) and the enhancement (positive), at best simultaneously on the same cluster. Up to now, only two groups (Andreani et al., 1996a, 1998; Holzapfel et al., 1997) have measured also the positive side of the signal at the only wavelength accessible from the ground (i.e. with enough transparency): 1.2 mm.

2. Our Instrument

The Italian group of the III University of Rome have built a photometer with two channels centred at 1.2 and 2 mm to feed the O.A.S.I. (Osservatorio Antartico Submillimetrico Infrarosso) telescope installed at the Italian base in Antarctica (Dall'Oglio et al., 1992). This photometer was adapted to be placed at the focus of the SEST antenna in Chile. The 2-mm band includes the peak brightness of the decrement in the S-Z thermal effect, while the 1.2-mm bandwidth is a compromise between the maximum value of the enhancement in the S-Z and the atmospheric transmission. The field of view in the sky was 44" at both frequencies. The beam separation in the sky was limited by the antenna chopping system and was set to the maximum chopping amplitude: 135".

Responsivities, beam shapes and widths were measured with planets and the sensitivity measured at the focus was: 7.5 mK/s at 1.2 mm and 10.7 mK/s at 2 mm. This means that in terms of relative change of the thermodynamic temperatures in one second integration time, we have $\left(\frac{\Delta T}{T}\right) = 0.01$ and 0.007 at 1.2 and 2 mm respectively.

3. The Choice of the X-Ray Clusters

Candidate sources were selected from the ROSAT southern clusters according to the following prescriptions: (a) high X-ray luminosity and (b) redshift larger than 0.25. This choice matches the two fundamental requirements: a small apparent angular dimension of the cluster core and a large Comptonisation parameter. The cluster angular dimensions should not largely exceed the instrument beam width and they

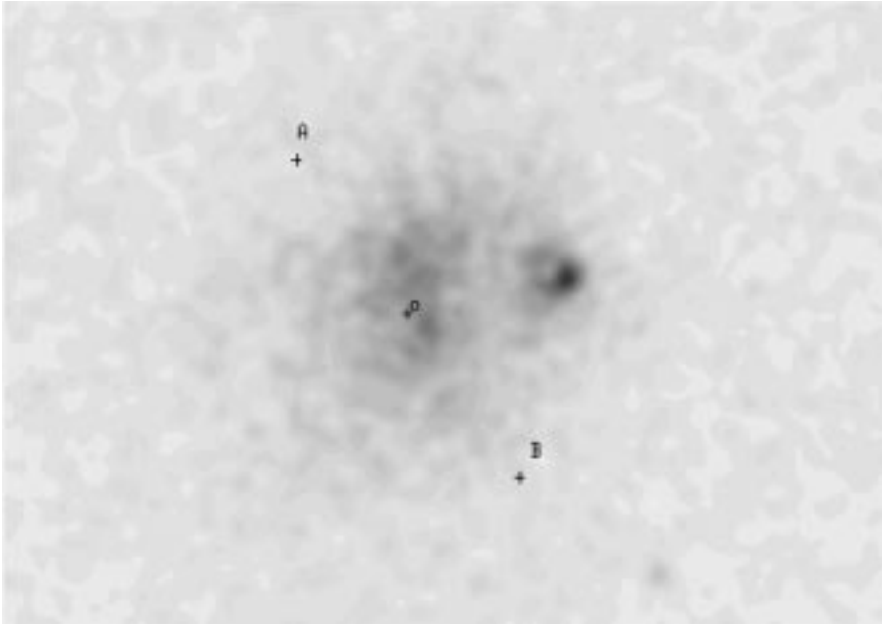


Figure 1: The ROSAT/PSPC X-ray image of RXJ0658-5557. The position of the central beam (o) and the reference beams (A and B) are shown as crosses superposed on the X-ray image. (Courtesy of Hans Böhringer). Field size is 17 arcmin in RA (horizontal axis) and 10 arcmin in declination (vertical axis). The redshift of the cluster is 0.31. The ROSAT count rate in the range 0.1 to 2.4 keV is 0.50 ± 0.04 per second.

must be smaller than the maximum chop throw, otherwise the amplitude of the signal cannot be correctly estimated. A large y parameter enhances the amplitude of the effect and therefore its detectability. Figure 1 shows superposed to the X-ray map of RXJ0658-5557 the location of the main beam (at the centre) with the reference beam (position A and B). Beam switching + nodding provides the real-time comparison between the emission from the cluster centre and that from the reference beams A and B.

As it is clear from the figure, the limited chop throw of the focal plane system did not allow us to measure the difference ON-OFF the cluster with the maximum sensitivity. This problem can be successfully tackled only using a wobbling secondary mirror, which is one of the foreseen upgrades of SEST mentioned before.

4. The Observations of the S-Z Enhancement and Decrement

Observations were collected in September 1994 and 1995 towards the X-ray clusters S1077, A2744, S295 and RXJ0658-5557. Description and performance of the instrument were reported in Pizzo et al. (1995) and in *The Messenger* No. 78 (1994), observations in Andreani et al. (1996a, 1996b and 1998).

Detections were found for A2744 at 1 mm and in both channels (at 1.2 and 2 mm) towards RXJ0658-5557. For the first time there was evidence for the S-Z enhancement and both the latter and the decrement were detected on the same source.

Observations of RXJ0658-5557 were carried out in four different nights during September 1–5, 1995. During the observations the sky opacity was very low ($\tau_{1\text{mm}} < 0.1$ with an average value of $\langle \tau_{1\text{mm}} \rangle = 0.07$, $\tau_{2\text{mm}} < 0.05$ with an average value of $\langle \tau_{2\text{mm}} \rangle = 0.03$) and the sky emission very stable thus producing a very low sky-noise. A total integration time of 12,400 s was spent on RXJ 0658-5557 and the same integration time was spent on a blank sky located 15 min ahead in right ascension with respect to the source position.

The effect we are looking for is very weak. We had therefore to check carefully all the systematics which could affect the measurements. Spill-over from the ground, difference in temperature from one side to the other of the main mirror and other effects could certainly plague the observations. Since it is hard to identify and quantify each effect, we measured them according to the following observing strategy: the source was integrated over time chunks of 600 s, this time interval plus the needed overheads gives a total tracking time on the source of 15 minutes. The same time was spent on a blank sky located with equatorial co-ordinates 15 minutes larger in right ascension. This means that the antenna tracked twice the same sky position in horizontal co-ordinates: once ON the source and the second time on the reference blank sky position. This enabled us to compare the two different measurements and eliminate the spurious signals.

Data were then extracted for the ON and OFF positions and the final estimate of the antenna temperature produced by the S-Z signal is given by $\Delta T_{\text{SZ}} = \Delta T_{\text{ON}} -$

ΔT_{OFF} . From a maximum likelihood analysis of the data ΔT_{SZ} we could infer an estimate of the antenna temperature at the two wavelengths: $\Delta T_{1\text{mm}} = + 0.3 \pm 0.06$ mK, $\Delta T_{2\text{mm}} = -0.46 \pm 0.13$ mK.

5. mm and X-Ray Data: Modelling the Hubble Constant

The angular diameter distance to a cluster can be observationally determined by combining measurements of the thermal S-Z effect and X-ray measurements of thermal emission from intra-cluster (IC) gas as shown in equations 2–6 above. While the physical basis is very simple and straightforward, the procedure to estimate the Hubble constant is still affected by large uncertainties. On the one hand, the radio, mm and sub-mm are plagued by the presence of discrete sources and/or diffuse dust in clusters. On the other hand, we still lack a deep knowledge of the distribution of the hot gas and its temperature in the cluster core. The X-ray image modelling involves several steps, each of them contains a source of unknown systematics. The final result is therefore affected by large uncertainties.

Here we show how we did proceed to estimate the luminosity distance to the cluster RXJ0658-5557 by combining the ROSAT X-ray image, the ASCA spectrum and the SZ mm observations.

5.1 Modelling the X-ray data

Our method consists of computing the expected S-Z map from the X-ray observations. This modelling requires the following steps:

(1) the construction of a X-ray surface brightness model fitting the X-ray image. This procedure allows to infer the physical parameter of the e^- gas, i.e. n_e .

(2) T_e is usually determined from the X-ray spectrum of the hot gas. In our case we made use of the ASCA GIS data. The temperature distribution is assumed to be isothermal and symmetrical.

(3) The distribution of the e^- density and temperature are then used to predict the expected S-Z increment and decrement: a map of the comptonisation parameter, y , is then built.

(4) Since the observed S-Z signal is the true one modified by the telescope primary beam and the beam switching, the predicted y -parameter is convolved with beam pattern and throw. These latter were measured during the calibration phase of the instrument. The convolved y -parameter is hereafter called Y .

5.2 A value for H_0

The numerical values in the modelling of the X-ray data depend on the Hubble parameter, H_0 , and in this way by comparing the predicted with measured values an estimate of the absolute distance of the cluster and H_0 can be made.

Hence the predicted versus observed Y-parameter are for the 2-mm channel:

$$\begin{aligned} (Y)_{X\text{-ray}} &= -2.73 \cdot 10^{-4} h_{50}^{-1/2} \\ (Y)_{\text{obs}} &= -2.53 \cdot 10^{-4} \end{aligned} \quad (7)$$

giving a formal result of the Hubble constant of $H_0 = 58^{+35}_{-22} \text{ km s}^{-1} \text{ Mpc}^{-1}$.

As the reader is aware, the error bars are quite large. They take into account many uncertainties still involved in this kind of measurements: the pointing position of the SEST and ROSAT Telescopes, the X-ray modelling and the uncertainties of the mm observations. These latter consider also the fact that the 1.2-mm channel is very likely affected by secondary cluster emission, maybe due to intracluster dust and/or sources.

The only way to get rid of these systematics is the observation of many clusters. Every source in fact contributes in a different way to the various modelling steps so that it is reasonable to assume that the average value of the

Hubble constant is a fair estimate of the real one.

This project would never have become a reality without the work of many people, among them I would like to thank my collaborators (H. Böhringer, R. Booth, G. Dall'Oglio, R. Lemke, L. Martinis, L.-Å. Nyman, A. Otàrola, L. Pizzo, P. Shaver, N. Whyborn), the SEST team and the Infrared group at La Silla and in particular Glenn Persson, Roland Lemke, Angel Otàrola, Peter de Bruin, Cathy Horellou, Peter Sinclair and Nicolas Haddad for their fundamental help and assistance during the observations and during the photometer set-up. This work has been partially supported by the P.N.R.A. (Programma Nazionale di Ricerche in Antartide). P.A. warmly thanks ESO for their hospitality during 1995, when part of this work was carried out.

References

Andreani P., Dall'Oglio G., L. Martinis, Böhringer H., Shaver P., Lemke R., Pizzo

L., Nyman L.-Å. Booth R., Whyborn N 1996a, in *Proceedings of the XVIth Moriond Astrophysics Meeting*, Les Arcs, France, March 1996a, eds. Bouchet F.R., Gisbert R., Guiderdoni B., p. 371.
 Andreani P. Pizzo L. Dall'Oglio G., Whyborn N., Böhringer H. Shaver P., Lemke R., Otàrola A., Nyman L.-Å. Booth R. 1996b, *ApJ* 459, L49
 Andreani P., Böhringer H., Dall'Oglio G., Martinis L., Shaver P., Lemke R., Nyman L.-Å., Booth R., Pizzo L., Whyborn N. Tanaka Y., Liang H., 1998, *ApJ* submitted.
 Birkinshaw M., 1997, *Physics Reports*, in press.
 Dall'Oglio et al., 1992, *Exp. Astron.* 2, 256.
 Holzapfel, W.L., Ade, P.A.R., Church, S.E., Mausekopf, P.D., Rephaeli, Y., Wilbanks, T.M. & Lange, A.E. 1997, *ApJ* 480, 449.
 Pizzo L., Andreani P., Dall'Oglio G., Lemke R., Otàrola A. and Whyborn N., 1995, *Exp. Astron.* 6, 249.
 Sunyaev R.A. and Zeldovich Ya B., 1972, *Comm. Astroph. Space Phys.*, 4, 173.

P. Andreani
 andreani@pd.astro.it

Cold Dust in Galaxies

R. CHINI¹, E. KRÜGEL²

¹*Astronomisches Institut der Ruhr-Universität Bochum, Germany*

²*Max-Planck-Institut für Radioastronomie, Bonn, Germany*

Abstract

The activity of galaxies reaches from the enhanced star-formation rate to the outburst of quasars. These different aspects of converting cold gas into luminosity can be well described by the ratio of infrared luminosity versus gas mass. The process of star formation is characterised by $L_{\text{IR}}/M_{\text{gas}}$ values of 5 [L_{\odot}/M_{\odot}] in normal spirals and 100 in active Mkn galaxies while quasars attain values above 500 due to additional non-thermal processes. Moreover, the coldest dust component in extragalactic objects also seems to be correlated with the stage of activity: T_{d} increases from 15 K in normal spirals to more than 40 K in quasars. New *ISOPHOT* data between 60 and 200 μm and SEST data at 1300 μm corroborate these results for active galaxies but indicate the presence of very cold dust (≈ 10 K) in normal spirals. The implications on the total gas content of galaxies are discussed. It turns out that high-resolution submm measurements of the dust emission with high spatial and spectral resolution play a key role for our understanding of the interstellar medium in external galaxies. In this context, plans for SIMBA, a new 37-channel bolometer array at 1300 μm for the SEST and the need for the LSA are briefly discussed.

1. Activity in Galaxies

In a previous *Messenger* article (Chini and Krügel, 1996, hereafter Paper I) we have described our long-term project on the global star-formation efficiency in various classes of galaxies. Our approach to this problem was the following: The energy of most galaxies originates from the formation of stars; only a few exotic objects like radio galaxies and quasars contain additional sources of energy which probably originate from the accretion of interstellar matter onto a circumnuclear disk. However, both sources of energy have in common that cold interstellar gas is transformed into luminosity. Therefore, the amount of luminosity obtained per unit gas mass, i.e. the ratio L/M_{gas} , should be an appropriate description for the activity in galaxies.

In order to obtain this ratio, we determined the two fundamental quantities L and M_{gas} for three samples of normal spirals, active galaxies and radio-quiet quasars. The total luminosity was approximated by the IR luminosity between 12 and 1300 μm . This interval is nicely covered by the infrared satellite *IRAS* at the wavebands 12, 25, 60 and 100 μm ; beyond that we managed to obtain the 1300- μm continuum flux from

the 15-m SEST or the 30-m IRAM telescope. The luminosity L_{IR} derived in this way is typically a factor of 10 higher than the blue luminosity L_{B} , indicating that it is a good approximation for the total luminosity of these objects.

The gas content M_{gas} of the galaxies was determined from the optically thin emission of dust at 1300 μm observed at the SEST and at IRAM. To convert the observed dust emission into a gas mass we used the fact that in the Milky Way, the amount of gas is about 150 times larger than that of dust. An independent check of the gas mass was derived from CO measurements: the intensity of the lower rotational levels J(1-0) and J(2-1) at wavelengths of 2.6 mm and 1.3 mm, respectively, has been verified empirically to be proportional to the mass of molecular hydrogen. The corresponding observations have also been performed at the SEST and the IRAM 30-m telescope. The major results of these studies as outlined in Paper I can be summarised as follows:

1. In normal spirals the spectral energy distribution from 100 to 1300 μm is dominated by cold dust of $T_{\text{d}} = 15 \pm 5$ K. Their gas mass is $2 \cdot 10^9 \leq M_{\text{gas}} \leq 6 \cdot 10^{10} M_{\odot}$ and their IR luminosity is $6 \cdot 10^9 \leq L_{\text{IR}} \leq 3 \cdot 10^{11} L_{\odot}$ yielding a ratio $L_{\text{IR}}/M_{\text{gas}} = 5 \pm 2$ in solar units.